Introduction to Robotics Lab 1

Karin Dyer, Saibernard Yogendran

Method

The FRANKA Emika Panda arm was visualized in the symbolic representation with the z axis (Figure 1)

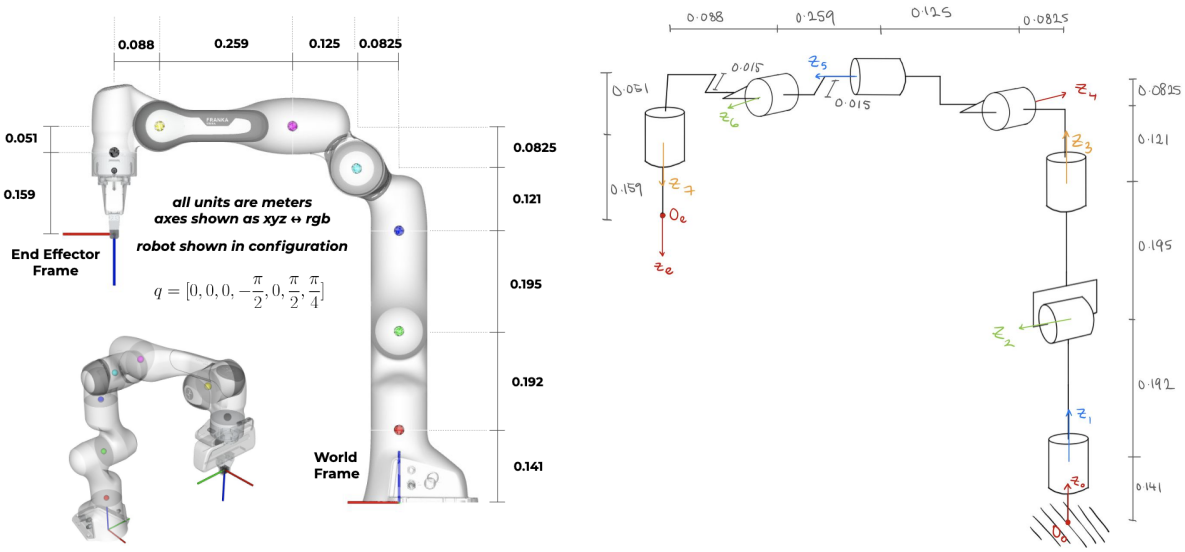

Figure 1: Symbolic representation of FRANKA Emika Panda Arm

Frames were then assigned to each link according to the DH convention (Figure 2)

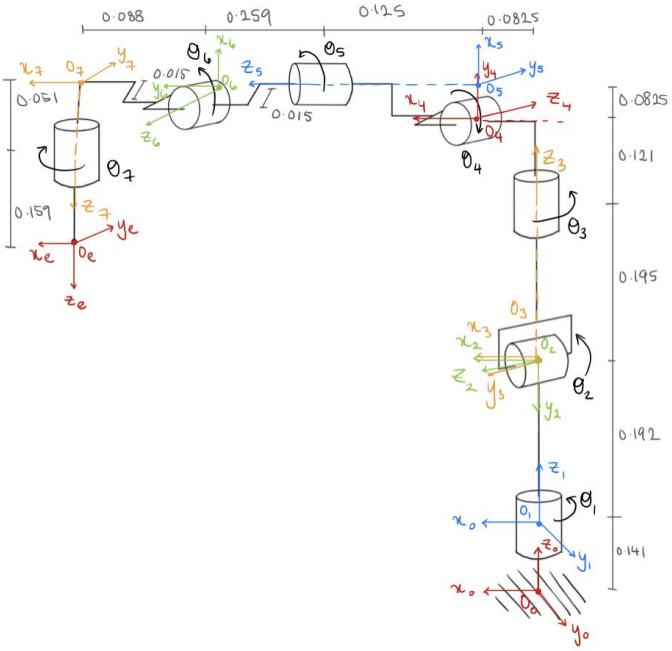

Figure 2: Symbolic representation of FRANKA Emika Panda arm with assigned frames

The values a_i α_i d_i and θ_i for each link were found according to the DH convention and are shown in Table 1. Where a_i is the distance between z_{i-1} and z_i along the x_i axis, α_i is the angle from z_{i-1} to z_i measured about x_i, d_i is the distance between x_{i-1} and x_i measured along the z_{i-1} axis, and θ_i is the angle from x_{i-1} to x_i measured about z_{i-1}.

Table 1: DH table

Link	a_i	α_i	d_i	θ_i
1	0	0	0.141	0
2	0	$-\frac{\pi}{2}$	0.192	θ_1
3	0	$\frac{\pi}{2}$	0	θ_2
4	0.825	$\frac{\pi}{2}$	0.316	θ_3
5	0.825	$\frac{\pi}{2}$	0	$\theta_4 - \pi$
6	0	$\frac{\pi}{2}$	0.384	θ_5
7	0.088	$-\frac{\pi}{2}$	0	$\pi - \theta_6$
8	0	0	0.210	$\theta_7 - \frac{\pi}{4}$

Code: (Saibernard's)

The values from Table 1 were stored in arrays of a_i α_i d_i and θ_i. The A_i matrices from 1 - 8 were created according to the layout in Figure 3 and pulled the values from the corresponding values in each array. The transformation matrices were calculated for each joint using matrix multiplication where:

$$T_n^0 = A_1 A_2 A_3 \ldots A_n$$

$$A_i = \begin{bmatrix} c_{\theta_i} & -s_{\theta_i}c_{\alpha_i} & s_{\theta_i}s_{\alpha_i} & a_i c_{\theta_i} \\ s_{\theta_i} & c_{\theta_i}c_{\alpha_i} & -c_{\theta_i}s_{\alpha_i} & a_i s_{\theta_i} \\ 0 & s_{\alpha_i} & c_{\alpha_i} & d_i \\ 0 & 0 & 0 & 1 \end{bmatrix}$$

Figure 3: A_i matrix layout

T_e^0 was stored in the variable T0e as one of the function outputs.

For frames with origins located elsewhere from the center of the corresponding joint (joints 3, 5, 6 and 7), the position of the center of the joint was found by multiplying the A_i matrix by a matrix corresponding to the offset in the x, y, and z direction with respect to the previous frame. The resulting matrix was transposed to fit the 1x3 joint position shape. For the remaining transformation matrices, the translational component (the first 3 rows of the last column) was extracted and stored as a 1x3 joint position matrix. These joint position arrays were stored in a stacked array called jointPositions as the other output of the forward function.

Evaluation

To further evaluate the accuracy of the simulation, we ran the forward function with the zero joint angles and different combination of other joint angles:

$q = [0,\ 0,\ 0,\ -\frac{\pi}{2},\ 0, \frac{\pi}{2},\ \frac{\pi}{4}]$

$q = [\frac{\pi}{2},\ 0,\ \frac{\pi}{4},\ -\frac{\pi}{2},\ -\frac{\pi}{2}, \frac{\pi}{2},\ 0]$

$q = [0,\ 0,\ 0,\ -\frac{\pi}{2},\ 0, \frac{\pi}{2},\ 0]$

The theoretical transformation matrix T_e^0 was as follows and the simulated end effector position for zero joint position is shown in Figure 4.

1.00	0.00	0.00	0.55
0.00	-1.00	0.00	0.00
0.00	0.00	-1.00	0.52
0.00	0.00	0.00	1.00

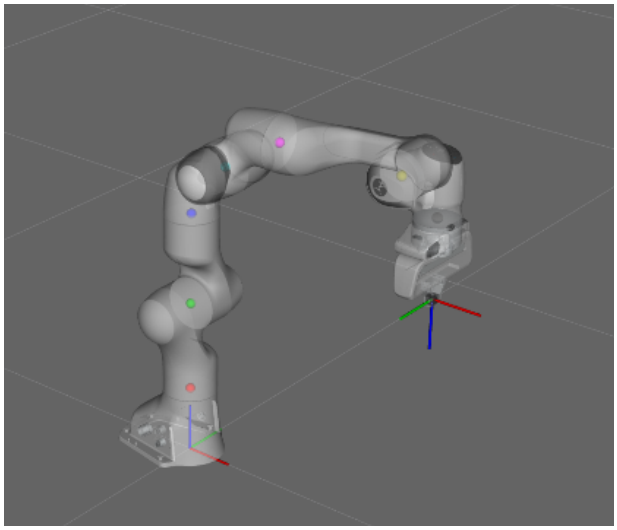

Figure 4: Simulated end effector position in zero joint position

Figure 5 and 6 represent the second and third joint configurations simulated positions and their end effector transformation matrix is shown:

-0.50	-0.50	0.71	0.24
0.50	0.50	0.71	0.54
-0.71	0.71	0.00	0.73
0.00	0.00	0.00	1.00

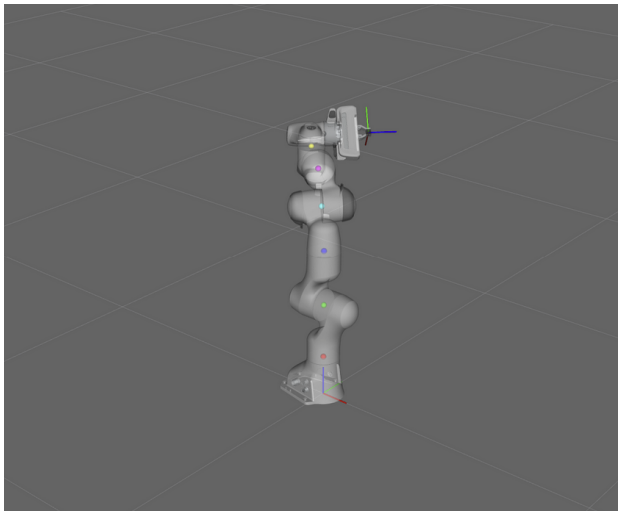

Figure 5: Simulated end effector position in second configuration

0.71	0.71	0.00	0.55
0.71	- 0.71	0.00	0.00
0.00	0.00	-1.00	0.52
0.00	0.00	0.00	1.00

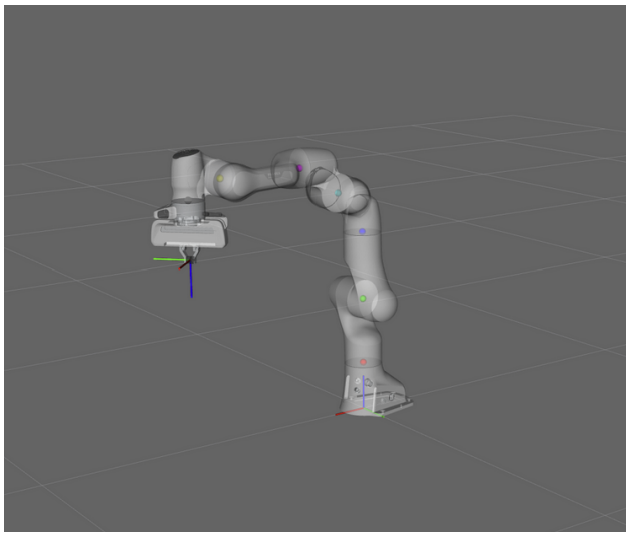

Figure 6: Simulated end effector position in third configuration

In comparing the generated T_e^0 matrix with all the simulated positions, the first 3 rows and 3 columns represent the rotational matrix and the first 3 rows of the last column represent the translational matrix. For the zero position, the rotational matrix tells us that the x axis of the end effector is aligned with the x axis of the world frame, the y axis of the end effector points in the negative y direction of the world frame, and the z axis on the end effector points in the negative z direction of the world frame. Similarly, the remaining configurations also match their transformation matrix with the simulated positions. As the simulated parameters for all the three configurations matched the theoretical, we felt confident that the code would work in hardware.

To further evaluate the accuracy, we tested the simulation and the hardware configuration and compared both. The FRANKA Emika Panda arm was arranged in the zero joint configuration and the end effector position was measured. The measurements were taken along the z axis of the world frame. The measurements are shown in Table 2.

Table 2: Theoretical and Physical measurements of FRANKA Panda Arm for different configurations

Joint Configuration (q)	Theoretical z (m)	Physical z (m)
$[0,\ 0,\ 0,\ -\frac{\pi}{2},\ 0,\frac{\pi}{2},\ \frac{\pi}{4}]$	0.520	0.516
$[\frac{\pi}{2},\ 0,\ \frac{\pi}{4},\ -\frac{\pi}{2},\ -\frac{\pi}{2},\frac{\pi}{2},\ 0]$	0.73	0.737
$[0,\ 0,\ 0,\ -\frac{\pi}{2},\ 0,\frac{\pi}{2},\ 0]$	0.52	0.511

The first joint configuration was chosen to verify the end effector position in the zero joint position as was done previously in the simulation. The second and third joint configurations were chosen due to the changes in the revolute joints. This rotation allows us to check the direction of rotation for the revolute joints with respect to the world frame. The same configurations that were simulated were used as input in the physical robot and the transformation matrix was verified. As the theoretical results match closely with the physical results, we can confidently say the simulation is an accurate representation of the real world. The small discrepancies between the theoretical and physical values are due to human measurement error.

Reachable Workspace

The reachable workspace of a manipulator is a set of all points the manipulator can reach. To capture this, we stored the upper and lower limits of each joint in a matrix. For each joint starting at joint 7, we iterated through a set of 5 evenly spaced values spanning the range of possible joint angles. The length of the array was set to 5 to capture the range of points while keeping the program runtime reasonable. The nested for loop runs the first iteration through joints 1 - 7 and after each iteration, the forward kinematics function is called with the q input being the set of generated joint angles. The loop plots each point as it's generated, with the first points being:

$$[joint1_0, joint2_0, joint3_0, joint4_0, joint5_0, joint6_0, joint7_0]$$
$$[joint1_0, joint2_0, joint3_0, joint4_0, joint5_0, joint6_0, joint7_1]$$
$$\dots$$
$$[joint1_0, joint2_0, joint3_0, joint4_0, joint5_0, joint6_0, joint7_4]$$

Once joint 7 has iterated through the loop, joint 6 begins its iteration. With each iteration of joint 6, the following loop must iterate through all of the 4 values of joint 7. This will plot points:

$$[joint1_0, joint2_0, joint3_0, joint4_0, joint5_0, joint6_1, joint7_{0-4}]$$
$$[joint1_0, joint2_0, joint3_0, joint4_0, joint5_0, joint6_2, joint7_{0-4}]$$
$$\dots$$

$$[joint1_0, joint2_0, joint3_0, joint4_0, joint5_0, joint6_4, joint7_{0-4}]$$

This nested loop continues for each joint, with the following joint iterating to completion with each 1 iteration of the previous joint. This gives us a full range of possible points the end effector will reach as each joint spans from one edge of its limit to the other. The resulting 3D reachable workspace of the manipulator is shown in Figure 7.

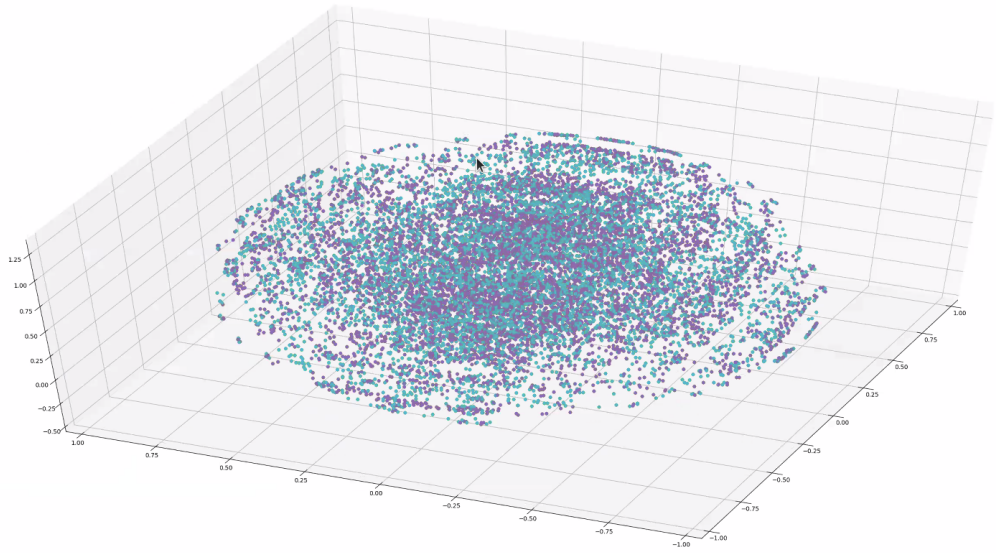

Figure 7: Reachable workspace of FRANKA Emika Panda arm

Analysis

The results were as expected with the only difference being the small discrepancy between the physical joint measurements and the simulated measurements. If the physical joint measurements were taken with sensors, the accuracy would be improved between the physical and the simulation.

The theoretical workspace does not have joint limitations, therefore it can encompass a larger workspace than the simulated. The simulated workspace is constricted to be within each joint's angle limit and represents the actual workspace of the physical robot. In our theoretical system, the physical joint limitations were incorporated, so the theoretical and simulated workspaces match. This workspace was also reflected in the physical workspace, meaning our code, simulation, and the physical robot, were representative of each other.

The workspace of the end effector in Figure 7 shows areas with less density than other areas. This may be due to the limited number of points each joint moved through. For the sake of program runtime, the loop took 5 points linearly spaced between the upper and lower limits for each joint. If this number was increased, the reachable workspace in Figure 7 would be more conclusive.

In the lab, we faced two hurdles from software to hardware. After successfully testing the code in simulation, the first robot did not respond to any commands due to a software issue in the physical robot. After connecting with the second robot, the roslaunch did not execute due to an error of network loss. The TA adjusted the communication cable to the robot and the roslaunch was successfully executed. From this we can understand that even though the simulated system may run successfully, the hardware system must be working properly to execute the code.

Differences between the simulated and physical robot include the reported joint positions. In the simulation the x, y, and z values are accurately recorded. However, the physical robot must be measured by hand. We learned that if sensors were incorporated to record the joint positions in the world frame, the software to hardware hurdle would be addressed. Furthermore, the hardware of the robot is subject to tolerances, an example being the degree tolerance of the motors in the joints. This may cause some discrepancies between the simulated positions and the physical positions.

We were able to derive the theoretical values of the FRANKA Emika Panda end effector. The theoretical joint positions for different joint configurations were verified with the simulation, and the physical robot. The hardware component of the lab was necessary to verify our theoretical calculations and understand the real world applications of forward kinematics.